IL NUOVO CIMENTO Online First
DOI 10.1393/ncb/i2007-10415-6

Laser cooling of solids: New results with single fluoride crystals

S. Bigotta([1])([*]), A. Di Lieto([1]), A. Toncelli([1]), M. Tonelli([1]),
D. Seletskiy([2]), M. P. Hasselbeck([2]), M. Sheik-Bahae([2]) and R. I. Epstein([3])

([1]) *INFN, Sezione di Pisa and Dipartimento di Fisica dell'Università Largo B. Pontecorvo 3, 56127 Pisa, Italy*
([2]) *Optical Science and Engineering Program, Department of Physics and Astronomy University of New Mexico - Albuquerque, NM 87131*
([3]) *Los Alamos National Laboratory - Mail Stop D436, Los Alamos, New Mexico 87545*

(ricevuto il 31 Dicembre 2007; approvato l' 11 Gennaio 2008; pubblicato online il 14 Aprile 2008)

Summary. — In the last decade, laser cooling of solids has evolved from an exotic scientific curiosity into a promising and challenging technology, thanks to the improvements in the crystal growth technologies and to innovative pumping schemes. We report the recent progress in the field obtained with fluoride single crystals doped with Tm and Yb. High optical quality fluoride single crystals allowed us to reach cooling efficiency as high as 3%. By using a resonant pumping cavity, a temperature drop of $\sim 70\,\mathrm{K}$ was observed. The room for improvements lets us think that temperature drops even larger than 100 K can be achieved.

PACS 42.55.Rz – Doped-insulator lasers and other solid state lasers.
PACS 78.55.Hx – Other solid inorganic materials.
PACS 81.10.Fq – Growth from melts; zone melting and refining.

1. – Introduction

The first experimental evidence of the laser cooling of solids was given by Epstein *et al.* [1] one decade ago, when the authors succeeded in cooling an Yb-doped fluorozirconate glass (ZBLANP) by anti-Stokes luminescence. Since then, many researchers have shown an interest in this field trying to increase the observed temperature drop from few fractions of K up to hundreds of K. Being the temperature drop proportional to the ratio of the surface area to the absorbed power, *i.e.* to the length of the sample, Mungan *et al.* [2] used a $250\,\mu$m ZBLAN diameter fiber instead of a more massive piece in order to optimize the cooling performance. Owing to this idea, a temperature drop of 16 K starting from room temperature was observed by pumping the fiber with 790 mW. Using a similar set-up and a pump power of 1360 mW, Luo *et al.* [3] obtained a temperature drop of 21 K.

([*]) E-mail: bigotta@df.unipi.it

Unfortunately, this scheme has two big pitfalls. First of all, the use of a fiber instead of a massive sample is not suitable for practical application as the "optical refrigerator" [4], where a large mass is required to remove heat. Second, improvements are possible only increasing the power. In fact, this approach does not solve one of the major problems of laser cooling: the absorbed power is just a marginal fraction of the pump power.

To overcome this problem, a new scheme was proposed by Gosnell [5]. This scheme is similar to the previous ones, but the unabsorbed pump radiation coming out from the end of the ZBLANP fiber is collected and reinjected into the sample with the help of an external high reflector, increasing the absorbed power by a factor 2. Using 1485 mW of pump power, Gosnell reported a temperature drop of 65 K from room temperature.

Heeg *et al.* [6] used a different approach to increase the absorbed power by placing the cooling medium inside a laser cavity. By placing a $2 \times 2 \times 3\,\mathrm{mm}^3$ 2% Yb:ZBLAN inside a diode-pumped Yb^{3+}:$KY(WO_4)_2$ laser cavity, cooling of $\approx 6\,\mathrm{K}$ has been observed.

A more efficient pump recycling scheme has been recently reported by Thiede *et al.* [7]. Both faces of the cooling element were coated with a dielectric mirror to trap the pump light. One face of the mirror has a small ($< 1\,\mathrm{mm}$) pinhole to admit the laser beam and trap the light inside the sample. Using this scheme, a temperature drop of 88 K has been obtained by pumping a 8 mm long cylindrical fiber preform with a 8 mm diameter core of 2% wt Yb-ZBLANP with a power of 11 W. This is the lowest temperature ever obtained by laser cooling.

In the meanwhile, the successes obtained have pushed forward several groups to find new materials that could enhance the results of Yb-doped ZBLANP. Indeed, up to now the mostly investigated material for laser cooling is still the fluorozirconate glasses ZBLAN and the very similar ZBLANP. Although few other Yb-doped hosts have been found, several papers report how the search has been generally unfruitful (see for example ref. [8]). Indeed, even if a number of candidates for optical refrigeration have been identified, available samples often lack the sufficient purity in order to show net cooling. Up to now, bulk cooling in crystals has been measured only in Yb^{3+}:YAG and Yb^{3+}:$Y_2Si_2O_5$ [9]. The thermal and mechanical properties of these crystals may be advantageous for practical applications, however, the authors report that the cooling efficiency was not as high as in the Yb-doped ZBLAN glasses, and the temperature drops observed in a single-pass configuration were 0.36 and 1 K for Yb^{3+}:YAG and Yb^{3+}:$Y_2Si_2O_5$, respectively.

Finally, all the above-mentioned experiments employ Yb^{3+} as coolant. However, this does not mean that Yb^{3+} is the only possible choice. Indeed, the first rare-earth ion ever proposed was the Gd^{3+} by Yatsiv; furthermore, the use of a ionic dopant with a smaller gap between the ground- and the excited-state manifold should lead to a higher cooling efficiency. In fact, just after the discovey of the laser cooling effect in solids, Edwards *et al.* [10] suggested using Tm^{3+}:ZBLANP or Dy^{3+}:$LaBr_3$ as cooling materials. Only recently, however, thanks to the availability of powerful laser sources in the mid-infrared, the cooling of a Tm^{3+}-doped glass has been shown. Hoyt *et al.* [11] observed a temperature drop of 1.2 K from room temperature for a single pass of the pump beam in a Tm:ZBLANP sample. In a more refined experiment [12], the authors allowed the pumping radiation to multiply pass through the sample by placing the sample itself in a non-resonant cavity. Using this experimental set-up, the authors obtained a cooling of 19 K from room temperature.

A starting point in finding the right material is the observation that the anti-Stokes optical cycle is in principle a laser cycle run in reverse. This may suggest that a good laser host material could also be an efficient host for optical refrigerators. However, it is

TABLE I. – *Physical properties of ZBLAN, YAG, BaYF and YLF matrices, after ref.* [9, 22-26].

	ZBLAN	YAG	BaY_2F_8	$LiYF_4$
Crystal structure	amorphous	cubic	monoclinic	tetragonal
Density (g/cm^{-3})	4.33	4.53	4.97	3.99
Thermal expansion $(10^{-6}K)^{-1}$	26.5	7.8	17 *a*-axis 18.7 *b*-axis 19.4 *c*-axis	8.3 $\perp$ *c*-axis 13.3 *c*-axis
Thermal conductivity (W/mK)	0.9	13	6	6.3
Transparency range (μm)	0.2–7	0.25–5	0.125–12	0.18–6.7
Refractive index at 1 μm	1.5	1.83	1.51 (ave.)	1.4 (ave.)
Microhardness (Knoop)	225	1215	235–350	300
Effective phonon energy (cm^{-1})	506	630	350	450
Hygroscopic	YES	NO	NO	NO
Specific heat (J/gK)	0.596	0.59	0.5	0.79

evident that to obtain new fruitful materials, the skills, the knowledge, and the technology employed in crystal growth are of fundamental importance. Fluoride crystals have long been used as a laser host material [13, 14]. More recently, the substantial and successful growth of very high quality crystals allowed to obtain new interesting results with rare-earth–doped fluorides crystals [15-18]. In this paper we report the recent progress in the field obtained with single crystals doped with Yb^{3+} and Tm^{3+}, grown in a Czochralski furnace at the Physics Department of the Pisa University.

Starting from the mechanical and physical properties, and using the spectroscopic data we collected from our samples, the theoretical and experimental cooling efficiency of these materials are evaluated and compared with respect to those of ZBLAN. Finally a new pumping scheme is proposed, and the results obtained are evaluated.

2. – Physical properties

BaY_2F_8(BaYF) has a monoclinic crystalline structure with C_{2h}^3 ($C2/m$) symmetry group [19]. The reticular constants are $a = 0.6935\,\text{nm}$, $b = 1.0457\,\text{nm}$, $c = 0.4243\,\text{nm}$, with angle γ between the *a*-axis and the *c*-axis of 99.7°. The primitive cell contains two BaYF molecules. $LiYF_4$(YLF) compound has the scheelite structure with tetragonal system. It crystallizes in $I4_1/a$ ($C^6 4h$) space group, and the lattice parameters are $a = 0.5155\,\text{nm}$, $b = 1.068\,\text{nm}$ [20]. The most striking features of single fluoride crystals with respect of ZBLAN are the very low phonon energy ($\sim 350\,\text{cm}^{-1}$ for BYF [21] and $\sim 450\,\text{cm}^{-1}$ for YLF [22]) that makes it suitable for laser application in the near IR region, and the low thermal lensing. The mechanical and physical properties of the fluorozirconate glass ZBLAN are reported in table I and compared with that of the crystals under study in this paper (BaYF and YLF), as well as a promising oxide crystal, YAG. This table illustrates that fluoride crystals offer several important advantages compared to ZBLAN that make them attractive in laser cooling applications. Indeed, the lower phonon energy reduces the non-radiative decay rate of the quenching centers and indirectly leads to higher emission efficiency; the transparency at longer infrared wavelengths makes it less susceptible to deleterious radiative heat loading; the thermal conductivity is an order of magnitude higher; the slightly higher material hardness allows for better polishing and direct deposition of optical coatings and, finally, absence of hygroscopic nature guarantees a longer durability and higher efficiency.

Compared to YAG, fluoride crystals do not offer the same mechanical properties. Specifically, YAG crystals show a better thermal conductivity and a higher material hardness. However, the optical properties of fluoride crystals can largely compensate for. Indeed, we believe that the lower phonon energy, the broader transparency range and a lower refractive index can make fluoride crystals good competitors of ZBLAN over YAG.

3. – Experimental

The growth facility consists of a home-made Czochralski furnace with resistive heating and automatic optical diameter-control. Crystal growth was carried out in high-purity argon atmosphere in order to avoid contamination in the melt and, for Yb-doped crystals, a suitable amount of CF_4 gas was added in order to prevent reduction of the Yb^{3+} ions to Yb^{2+}. Indeed, this reduction may severely compromise the optical quality of the crystals. The temperature of the melt was around 995 °C for BaYF and 845 °C for YLF. During the growth, the rotation rate of the sample was 5 r.p.m. and the pulling rate was 0.5 mm/h and 1 mm/h for the BaYF and YLF, respectively. The crystals were grown using LiF-YF_3 and BaY_2F_8-BaF_2 powders as raw material for the crystal and the doping density was achieved by adding a proper amount of YbF_3 or TmF_3 powders. To avoid OH^- contamination, the powders were purified at AC Materials (Orlando, FL, USA), obtaining a purity of 99.999%. Special care has been devoted to the quality of the vacuum system, which has an ultimate pressure limit below 10^{-5} Pa. Using this apparatus 2.5% Yb:BaYF, 5% Yb:YLF and 1.2% Tm:BaYF have been grown.

The crystals were of high optical quality, free of cracks and micro-bubbles. The single crystalline character of the samples was checked using a X-ray Laue technique to identify the crystallographic axes of the crystal and cut oriented samples. For laser cooling experiments, small parallelepipeds have been cut and all the six faces were polished to a high optical quality.

The experimental set-up employed to obtain the absorption and emission spectra used in subsect. **4**˙1, has been described in a previous paper [27]. The apparatus used in the single-pass laser cooling experiments described in subsect. **4**˙2 consists of a laser emitting at an appropriate wavelength, whose output is focused onto the crystal. The crystal is placed in a small vacuum chamber and suspended on two crossed microscope cover slips in order to reduce parasitic heat loading from the surroundings, that is mainly due to conduction and convection mechanisms. For this reason, the vacuum inside the chamber was kept at pressures less than 10^{-1} Pa by use of a cryogenic or a turbo-molecular pump. To keep the heat load as low as possible, the temperature measurements were performed by using non-contact thermometry method. Both a thermal camera and a spectroscopic method have been employed to determine the temperature of the samples. The details about these methods, as well as the whole experimental set-ups may be found in refs. [27-29].

4. – Cooling results

4˙1. *Cooling potentialities*. – The basic processes involved in laser cooling have been extensively studied by several authors [1, 8, 11]. Here we only summarize the main concepts. By pumping an Yb^{3+} or Tm^{3+}-doped sample on the long-wavelength tail of the absorption spectrum, the ions are moved from the top of the ground state to the bottom of the excited state. Then, the ions thermalize within the manifold by rapid ($\tau \sim 10^{-12}$ s)

TABLE II. – *Cooling figures of merit $F_{\rm cool}$ of the hosts that showed bulk cooling.*

Material	$F_{\rm cool}$ (10^{-23}) cm^2	Ref.
Yb^{3+}:YAG	3.2	[9]
Yb^{3+}:YSO	1.5	[9]
Yb^{3+}:BaYF ($E \parallel b$, $H \parallel a$)	1.4	[this work]
Yb^{3+}:YLF ($E \parallel b$, $H \parallel a$)	1.4	[this work]
Tm^{3+}:BaYF ($E \parallel b$)	1.3	[this work]
Tm^{3+}:ZBLAN	1.1	[30]
Yb^{3+}:ZBLAN	0.7	[8]

absorption of phonons from the host and decay again to the ground state through spontaneous emission ($\tau \sim 10^{-3}$ s). In the ideal case, each fluorescent photon removes, on average, an amount of energy equal to the difference between the pump photon $h\nu$ and the mean fluorescent photon $h\nu_f$. By defining a cooling efficiency as the ratio between cooling power and absorbed power, one obtains

$$\eta_{\rm cool} = \frac{P_{\rm cool}}{P_{\rm abs}} = \frac{h\nu_f - h\nu}{h\nu} = \frac{\lambda - \lambda_f}{\lambda_f}\,. \tag{1}$$

Equation (1) states that if the material is pumped at longer wavelengths, the efficiency increases. It is clear, however, that moving further in the absorption tail will result in lower absorption, decreasing the absorbed power. For this reason, a more useful figure of merit of the cooling process should take also into account the absorption cross-section $\sigma_{\rm abs}(\lambda)$ at the pumping wavelength. If we define the wavelength-dependent quantity $F_{\rm cool}$ as the product of the cooling efficiency times the absorption cross-section

$$F_{\rm cool}(\lambda) = \sigma_{\rm abs}(\lambda)\eta_{\rm cool} = \sigma_{\rm abs}(\lambda)\frac{\lambda - \lambda_f}{\lambda_f}\,, \tag{2}$$

we see that this quantity is positive for $\lambda > \lambda_f$, may have one or more peaks, depending on the structure of the absorption spectrum, and then tends to zero for $\lambda \gg \lambda_f$, when the absorption becomes negligible. The maximum of $F_{\rm cool}$ may thus be used to evaluate the cooling potentiality of a host. In a more realistic model, one should take into account the percentage of radiation that is trapped in the crystal due to total internal reflection and the losses related to scattering, impurities and non-radiative decays (see, for instance, ref. [11] for a more refined model). Nevertheless, this simple model gives useful hints in searching a host for laser cooling, since $F_{\rm cool}$ can easily be calculated from absorption and emission spectra.

Table II summarizes the maximum values of the cooling figure of merit for the hosts employed in laser cooling experiments.

This table shows that the maximum $F_{\rm cool}$ for Yb:BaYF and Yb:YLF is 1.4×10^{-23} cm^2 and 1.3×10^{-23} cm^2 Tm:BaYF. These values are lower than that observed for oxide crystals, but are almost twice the 0.7×10^{-23} cm^2 reported for the Yb:ZBLANP glass and greater than that of Tm:ZBLAN. The higher values of $F_{\rm cool}$ are to be ascribed to the higher absorption cross-section of the crystals with respect to that of glasses, confirming the potentiality of this class of materials.

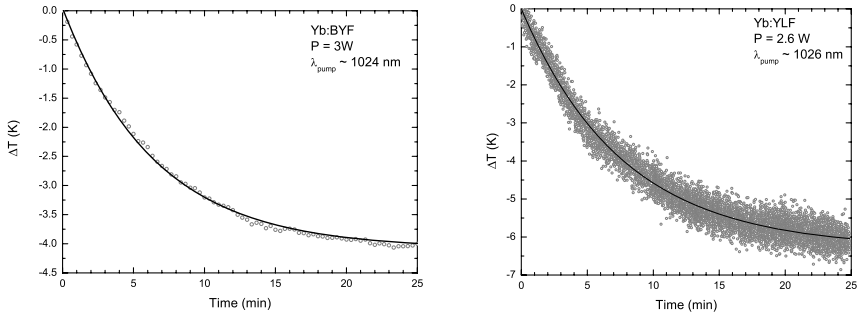

(a) (b)

Fig. 1. – Temporal behavior of cooling (dot) and theoretical exponential fit (line) for 2.5% Yb:BaYF (a) and 5% Yb:YLF (b).

4˙2. *Bulk cooling*. – Figure 1 shows the typical temporal evolution of cooling after the sample is irradiated. The temperature change is clearly exponential, as expected from simple thermodynamical considerations [31]. A maximum temperature drop of about 4 K starting from room temperature has been achieved in single-pass configuration when the Yb:BaYF is irradiated with 3 W at 1024 nm, the shortest available wavelength with our experimental set-up, while a temperature drop of 6.3 K when irradiated with 2.6 W at 1026 nm has been observed in Yb:YLF. The full potentiality of the Yb^{3+}-doped samples is still to be determined since we could not scan the whole cooling wavelength range, being limited by the restricted tunability range of the laser diodes. In fact, according to ref. [11], the maximum temperature drop is located somewhere at a wavelength longer than that of the maximum of F_{cool} (1015 nm), the exact value depending basically on the impurities in the sample. By pumping the crystal at a wavelength between 1015 and 1024 nm, we may expect to find a larger temperature drop.

In the case of Tm:BaYF the pump source was a home-made optical parametric oscillator [29]. This enables us to scan the whole interesting absorption region of Tm ions, that is from 1800 to 2050 nm, as shown in fig. 2. This figure shows that a maximum temperature drop of 6.6 W occurs when the sample is irradiated with 4.4 W at 1855 nm.

The importance of these results may be better highlighted if one considers the cooling efficiency obtained with single fluoride crystals. The cooling power extracted may be estimated if we consider that it must balance the incoming power in equilibrium conditions and that the heat loading on the sample is due to the radiation coming from the vacuum chamber only. We can then write

$$P_{\mathrm{cool}} = \epsilon_s \sigma A \big(T_c^4 - T_s^4\big), \tag{3}$$

where T_c and T_s are the temperature of the vacuum chamber and of sample, respectively, A is the area and ϵ_s the emissivity of the sample and σ is the Stefan-Boltzmann constant. Using eq. (3) a cooling efficiency of $\sim 3\%$ for the BaYF crystals and $\sim 2\%$ for Yb:YLF have been estimated. This indicates that the cooling efficiency of BaYF crystals is larger than the $\sim 2\%$ efficiency reported for both Yb:YAG [9] and Yb:ZBLANP [32] in single-pass configuration, confirming that this material could play an important role as a competitor of the fluorozirconate glasses. In the case of Yb:YLF, the $\sim 2\%$ efficiency may be ascribed to multiple absorption-reemission processes. Indeed, it is well known

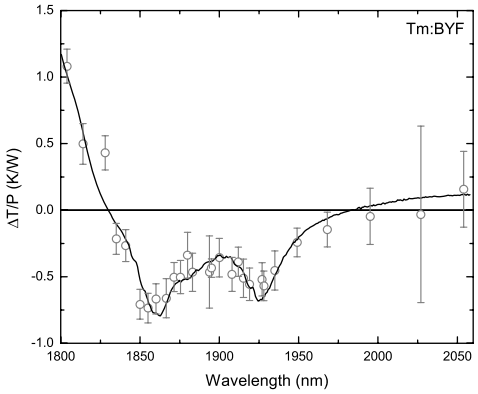

Fig. 2. – Wavelength-dependent temperature change normalized to pump power for BaYF doped 1.2% Tm for $E \parallel b$. Data points below the horizontal reference line indicate net cooling. The solid curve is a fit as described in the text.

that in a fluorescent solid part of the emitted light is trapped inside the body due to total internal reflection, reducing the external quantum efficiency, and that the amount of light trapped is proportional to the dopant concentration.

4˙3. *Enhanced cavity absorption.* – A novel method to increase the absorption of the cooled sample by trapping the pump light in it has recently demonstrated [33]. This method overcomes the shortcomings of the other non-resonant scheme, mainly due to the hole needed to couple the pump in the sample. This pumping scheme utilizes a cavity made of an input mirror of reflectivity R_{ic}, the intracavity cooling element with an absorption coefficient α and length l and a second high-reflectivity mirror. The power absorbed by the cooling element may be maximized by carefully choosing the input mirror of such a lossy cavity. Indeed, it can be shown [33] that the absorption is given by

$$A = \frac{1-\Delta}{1+F\sin^2\delta}, \text{ with } \Delta = \frac{(\sqrt{R_{ic}} - e^{-\alpha l})^2}{(1-e^{-\alpha l}\sqrt{R_{ic}})^2} \text{ and } F = \frac{4e^{-\alpha l}\sqrt{R_{ic}}}{(1-e^{-\alpha l}\sqrt{R_{ic}})^2} \tag{4}$$

and where δ is equal to kl, k being the wave vector inside the absorbing material. From the above equations it is clear that the absorption is maximum when Δ is zero, *i.e.* the fraction of absorbed power approaches to one. This happens when the reflectivity R_{ic} of the input mirror is equal to

$$R_{ic} = e^{-2\alpha l}. \tag{5}$$

The experimental set-up used for cavity enhanced resonant absorption cooling is shown in fig. 3. It consists of a commercial Yb:YAG thin-disk laser (ELS Versadisk) that can provide up to 45 W of c.w. power at 1030 nm. To avoid optical feedback that may cause lasing to be unstable, a Faraday isolator in combination with a high-isolation polarizing beam splitter and a quarter-wave plate were placed in front of the laser. Two mode-matching lenses ($f_1 = 50$ mm, $f_2 = 100$ mm) have been used to effectively couple pump

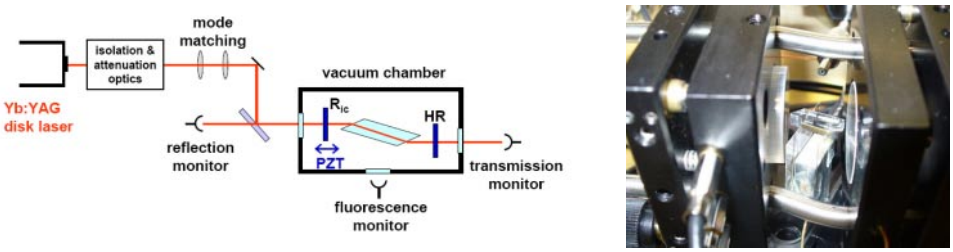

(a) (b)

Fig. 3. – Experimental set-up used in laser cooling experiments. (a) Scheme. Note that the feedback stabilization and control electronics are not shown in figure. (b) Detail of the cavity.

light to the TEM_{00} cavity mode. The resonant cavity is placed inside an aluminum vacuum chamber. The pump light enters through an AR-coated window. To allow for the cavity length scanning/tuning, the input mirror of the cavity, having reflectivity R_{ic}, is mounted on a 3-axis piezoelectric mirror mount. The second mirror, HR-coated, is mounted on a fixed holder. In order to minimize the losses due to Fresnel reflection, a Brewster cut sample has been used. The reflectivity of the cavity is monitored by a Si detector placed behind the last turning pump mirror. During laser cooling measurements the cavity is stabilized via an electronic feedback loop. The details about the feedback stabilization and control electronics will be given elsewhere. The results obtained with that cavity are shown in fig. 4. This figure shows the evolution of the temperature of the intracavity element, a 5% Yb:YLF single crystal, upon illumination by the pump laser with increasing pump powers (open circles), together with the temperature of the surrounding mirrors (full circles). During the times when the laser is on the sample the

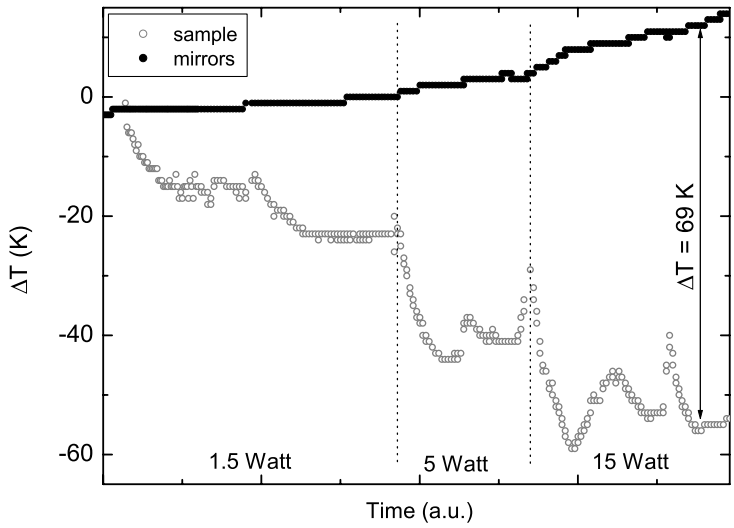

Fig. 4. – Temporal evolution of the temperature of the intracavity cooling element (5% Yb:YLF, open dots) and that of the surrounding mirrors (full dots) at different pumping powers.

cavity length is stabilized via the feedback loop. Noise, latency and imperfections in the feedback loop along with vibrations due to vacuum turbo-molecular pump lower the trapping efficiency and are responsible of the bumps on the curve at high power, when the sample is heated back by the mirrors while recovering the stabilization of the cavity. From this figure, a maximum temperature difference between the surrounding mirrors and the cooling sample of 69 K have been obtained, corresponding to an extracted power of 58 mW.

5. – Conclusion

The spectroscopic investigation together with the optical and mechanical properties confirm the good properties of fluoride single crystals for laser cooling applications. Single-pass cooling runs confirmed experimentally the goodness of these materials and showed that the cooling efficiency was as high as 3%. A new pumping scheme has been tested and a temperature drop of ~ 70 K with respect to the surrounding environment have been observed, corresponding to an extracted power of 58 mW.

* * *

The authors wish to thank I. Grassini for preparation of the samples and H. P. Jenssen and A. Cassanho that, thanks to their expertise in crystal growth developed at the AC Materials (Orlando, FL, USA), gave us precious suggestions.

REFERENCES

[1] Epstein R. I., Buchwald M. I., Edwards B. C., Gosnell T. R. and Mungan C. E., *Nature*, **377** (1995) 500.
[2] Mungan C. E., Buchwald M. I., Edwards B. C., Epstein R. I. and Gosnell T. R., *Phys. Rev. Lett.*, **77** (1997) 1030.
[3] Luo X., Eisaman M. D. and Gosnell T. R., *Opt. Lett.*, **23** (1998) 639.
[4] Edwards B. C., Buchwald M. I. and Epstein R. I., *Rev. Sci. Instrum.*, **69** (1998) 2050.
[5] Gosnell T. R., *Opt. Lett.*, **24** (1999) 1041.
[6] Heeg B., Stone M. D., Khizhnyak A., Rumbles G., Mills G. and DeBarber P. A., *Phys. Rev. A*, **70** (2004) 021401(R).
[7] Thiede J., Distel J., Greenfield S. R. and Epstein R. I., *Appl. Phys. Lett.*, **86** (2005) 154107.
[8] Bowman S. R. and Mungan C. E., *Appl. Phys. B*, **71** (2000) 807.
[9] Epstein R. I., Brown J. J., Edwards B. C. and Gibbs A., *J. Appl. Phys.*, **90** (2001) 4815.
[10] Edwards B. C., Buchwald M. I., Epstein R. I., Gosnell T. R. and Mungan C. E., in *Proceedings of the 9th Annual American Institut of Astronautics & Aeronautics Utah State Conference on Small Satellites*, edited by Redd F. (American Institut of Astronautics & Aeronautics) 1996.
[11] Hoyt C. W., Sheik-Bahae M., Epstein R. I., Edwards B. C. and Anderson J. E., *Phys. Rev. Lett.*, **85** (2000) 3600.
[12] Hoyt C. W., Sheik-Bahae M., Epstein R. I., Greenfield S., Thiede J., Distel J. and Valencia J., *J. Opt. Soc. Am. B*, **20** (2003) 1066.
[13] Johnson L. F. and Guggenheim H. J., *Appl. Phys. Lett.*, **23** (1973) 96.
[14] Jenssen H. P. and Cassanho A., in *Proceedings of SPIE - Photonics West* 6100-24 (2006).
[15] Vannini M., Toci G., Alderighi D., Parisi D., Cornacchia F. and Tonelli M., *Opt. Express*, **15** (2007) 7994.

[16] Cornacchia F., Richter A., Heumann E., Huber G., Parisi D. and Tonelli M., *Optics Express*, **15** (2007) 992.
[17] Tabirian A. M., Jenssen H. P. and Cassanho A., *Efficient, room temperature mid-infrared laser at 3.9 μm in* Ho:BaY_2F_8, in *OSA Proc. Advanced Solid-State Lasers, Trends in Optics and Photonics*, **50** (2001) 170.
[18] Galzerano G., Cornacchia F., Parisi D., Toncelli A., Tonelli M. and Laporta P., *Opt. Lett.*, **30** (2005) 854.
[19] Izotova O. E. and Aleksandrov V. B., *Sov. Phys. Dokl.*, **16** (1970) 525.
[20] Bensalah A., Guyot Y., Ito M., Brenier A., Sato H., Fukuda T. and Boulon G., *Opt. Mater.*, **26** (2004) 375.
[21] Toncelli A., Tonelli M., Cassanho A. and Jenssen H. P., *J. Lum.*, **82** (1999) 291.
[22] Orlovskii Y. V., Basiev T. T., Vorob'ev I. N., Orlovskaya E. O., Barnes N. P. and Mirov S. B., *Opt. Mater.*, **18** (2002) 355.
[23] Weber M. J., *Handbook of Optical Materials* (CRC Press) 2002.
[24] Jenssen H. P., personal communication (2005).
[25] Kaminskii A. A., *Phys. Status Solidi A*, **137** (1993) K61.
[26] Shikida A., Yanagita H. and Toratani H., *J. Opt. Soc. Am. B*, **11** (1994) 928.
[27] Bigotta S., Parisi D., Bonelli L., Di Lieto A., Toncelli A. and Tonelli M., *J. Appl. Phys.*, **100** (2006) 013109.
[28] Bigotta S., Di Lieto A., Parisi D., Toncelli A. and Tonelli M., in *Proceedings of SPIE - Photonics West* 64610E (2007).
[29] Patterson W., Bigotta S., Sheik-Bahae M., Parisi D., Tonelli M. and Epstein R. I., *Optics Express*, **16** (2008) 1704.
[30] Patterson W., personal communication (2007).
[31] Clark J. L., Miller P. F. and Rumbles G., *A*, **102** (1998) 4428.
[32] Fajardo J. C., Siegel G. H. jr., Edwards B. C., Epstein R. I., Gosnell T. R. and Mungan C. E., *J. Non-Cryst. Solids*, **213-214** (1997) 95.
[33] Seletskiy D., Hasselbeck M. P., Sheik-Bahae M., Thiede J. and Epstein R. I., in *Advanced Optical and Quantum Memories and Computing III Proc. SPIE*, **6130** (2006) 61300P.